

# Mesoscopic Rydberg Gate based on Electromagnetically Induced Transparency

M. Müller,<sup>1</sup> I. Lesanovsky,<sup>1</sup> H. Weimer,<sup>2</sup> H.P. Büchler,<sup>2</sup> and P. Zoller<sup>1</sup>

<sup>1</sup>*Institute for Theoretical Physics, University of Innsbruck,*  
*and Institute for Quantum Optics and Quantum Information of the Austrian Academy of Sciences, Innsbruck, Austria*  
<sup>2</sup>*Institute for Theoretical Physics III, University of Stuttgart, Pfaffenwaldring 57, 70550 Stuttgart, Germany*

(Dated: December 22, 2021)

We demonstrate theoretically a parallelized C-NOT gate which allows to entangle a mesoscopic ensemble of atoms with a single control atom in a single step, with high fidelity and on a microsecond timescale. Our scheme relies on the strong and long-ranged interaction between Rydberg atoms triggering Electromagnetically Induced Transparency (EIT). By this we can robustly implement a conditional transfer of all ensemble atoms among two logical states, depending on the state of the control atom. We outline a many body interferometer which allows a comparison of two many-body quantum states by performing a measurement of the control atom.

PACS numbers: 03.67.-a,32.80.Rm,42.50.Gy

Atoms excited by laser light to high-lying Rydberg states interact via strong and long-range dipole-dipole or Van der Waals forces [1]. Level shifts associated with these interactions can be used to block transitions of more than one Rydberg excitation in mesoscopic atomic ensembles. This “dipole blockade” [2] mechanism underlies the formation of “superatoms” in atomic gases with a single Rydberg excitation shared by many atoms within a blockade radius. Furthermore, this provides the basis for fast two-qubit gates between pairs of atoms in optical or magnetic trap arrays. Recently, these superatoms and Rydberg gates have been demonstrated in the laboratory by several groups in remarkable experiments [3, 4]. Building on these achievements, a future challenge is to develop and extend Rydberg-based protocols towards single step *many atom entanglement*. In this letter, we propose and analyze a fast high-fidelity many-particle gate by combining elements of EIT and Rydberg interactions, which entangles *in a single step* a control atom with a mesoscopic number of atoms  $N$ . Such a mesoscopic parallel Rydberg gate has immediate applications in entanglement-based many-particle interferometry, and in quantum information processing.

as in Ref. [4], or in large-spacing optical lattices or magnetic trap arrays [5]. Our goal is the implementation of the operation C-NOT <sup>$N$</sup> , defined by

$$\begin{aligned} |0\rangle|A^N\rangle &\rightarrow |0\rangle|A^N\rangle, & |0\rangle|B^N\rangle &\rightarrow |0\rangle|B^N\rangle, \\ |1\rangle|A^N\rangle &\rightarrow |1\rangle|B^N\rangle, & |1\rangle|B^N\rangle &\rightarrow |1\rangle|A^N\rangle, \end{aligned} \quad (1)$$

where  $|0\rangle$ ,  $|1\rangle$  and  $|A\rangle$  and  $|B\rangle$  denote long-lived ground states of the control and ensemble atoms, respectively. The gate consists of a conditional swap of the two internal states of  $N$  ensemble atoms depending on the state of the control, where we have adopted the notation  $|A^N\rangle \equiv \bigotimes_{k=1}^N |A\rangle_k$  and  $|B^N\rangle \equiv \bigotimes_{k=1}^N |B\rangle_k$ . The gate (1) corresponds to a Schrödinger-cat or GHZ-type beam splitter:  $(\alpha|0\rangle + \beta|1\rangle)|A^N\rangle \rightarrow \alpha|0\rangle|A^N\rangle + \beta|1\rangle|B^N\rangle$ . The resulting state constitutes an important resource for quantum computing, and provides a basic ingredient for Heisenberg limited interferometry [6].

The basic elements and steps in our realization of the gate (1) are: (i) in our setup the control atom can be individually addressed, and laser excited to a Rydberg state conditional to its internal state, thus (ii) turning on or off the strong long-range Rydberg-Rydberg interactions of the control with ensemble atoms, which (iii) via EIT-type interference suppresses or allows the transfer of all the ensemble atoms from  $|A\rangle$  or  $|B\rangle$  conditional to the state of the control atom. Among the distinguishing features of our protocol is high fidelity for moderately sized atomic ensembles that are spread out over a distance of several micrometers. It is robust with respect to inhomogeneous interparticle distances and varying interaction strengths and can be carried out on a microsecond timescale. Furthermore, we find that mechanical effects caused by the strong forces between Rydberg atoms will not spoil the fidelity of the gate operation.

Let us now discuss the concrete physical implementation of the gate (1). To this end we introduce intermediate states for the control and the ensemble atoms as shown in Fig. 2. In addition to the states  $|0\rangle$ ,  $|1\rangle$

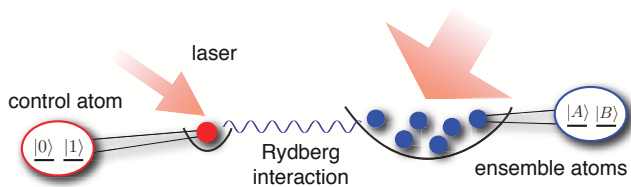


Figure 1: In the envisioned setup the quantum state of an atomic ensemble is manipulated depending on the state of a single control atom. The atomic ensemble can consist of atoms in a single trap or of atoms being confined in a lattice.

We envision a setup as illustrated in Fig. 1. A control atom and a mesoscopic ensemble of atoms are stored in two separate trapping potentials, e.g. in two dipole traps

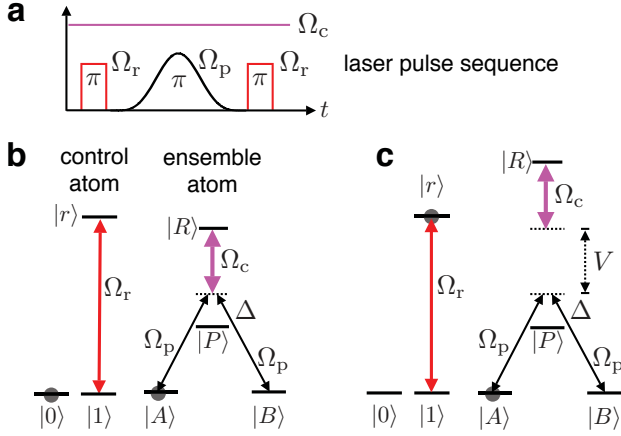


Figure 2: **a**: Sequence of laser pulses (not to scale). **b**: Electronic level structure of the control and ensemble atoms. The ground state  $|1\rangle$  is resonantly coupled to the Rydberg state  $|r\rangle$ . The states  $|A\rangle$  and  $|B\rangle$  are off-resonantly coupled (detuning  $\Delta$ , Rabi frequency  $\Omega_p$ ) to  $|P\rangle$ . A strong laser with Rabi frequency  $\Omega_c \gg \Omega_p$  couples the Rydberg level  $|R\rangle$  to  $|P\rangle$  such that  $|R\rangle$  is in two-photon resonance with  $|A\rangle$  and  $|B\rangle$ . In this situation (known as EIT) Raman transfer from  $|A\rangle$  to  $|B\rangle$  is inhibited. **c**: With the control atom excited to  $|r\rangle$  the two-photon resonance condition is lifted as the level  $|R\rangle$  is shifted due to the interaction energy  $V$  between the Rydberg states, thereby enabling off-resonant Raman transfer from  $|A\rangle$  to  $|B\rangle$ .

of the control atom we consider the Rydberg level  $|r\rangle$  which is resonantly coupled to the state  $|1\rangle$  by a laser with (two-photon)-Rabi frequency  $\Omega_r$ . In the rotating wave approximation the corresponding Hamiltonian reads  $H_r = [(\Omega_r/2)|1\rangle\langle r| + \text{h.c.}]$ . The ensemble atoms possess the two stable ground states  $|A\rangle$  and  $|B\rangle$ , the intermediate state  $|P\rangle$  and a Rydberg state  $|R\rangle$ . The state  $|P\rangle$  can be a p-state of an alkali metal atom, e.g.  $5^2P_{3/2}$  in case of  $^{87}\text{Rb}$ , and possesses a lifetime  $\gamma_p^{-1}$  of tens of nanoseconds. The ground states are off-resonantly coupled (detuning  $\Delta$ ,  $\Delta \gg \gamma_p$ ) to the intermediate state by two Raman lasers, which for simplicity are assumed to have the same Rabi frequency  $\Omega_p$  (see fig. 2b). A second laser with Rabi frequency  $\Omega_c$  ( $\Delta \gg \Omega_c > \Omega_p$ ) couples the states  $|R\rangle$  and  $|P\rangle$  such that the two ground states are in two photon resonance with the Rydberg state.

We will now outline the essence of the conditional transfer of the ensemble atoms from the state  $|A^N\rangle$  to  $|B^N\rangle$ . We consider first the case of non-interaction ensemble atoms since it can be treated in a simple single particle picture. Subsequently, we provide a discussion of the effects caused by the interaction among the ensemble atoms. First, we have to distinguish between the two cases in which the control atom is in state  $|0\rangle$  or  $|1\rangle$ . In the former case we intend to achieve a blocking of the transfer  $|A^N\rangle \rightarrow |B^N\rangle$  whereas in the latter case the transfer shall be enabled. In both cases the

same sequence of laser pulses sketched in fig. 2a is applied, i.e. a short  $\pi$ -pulse on the control atom, followed by a smooth Raman  $\pi$ -pulse  $\Omega_p(t)$  of duration  $T$  with  $\int_0^T dt \Omega_p^2(t)/(2\Delta) = \pi$  acting on the ensemble atoms, followed by a second  $\pi$ -pulse on the control atom.

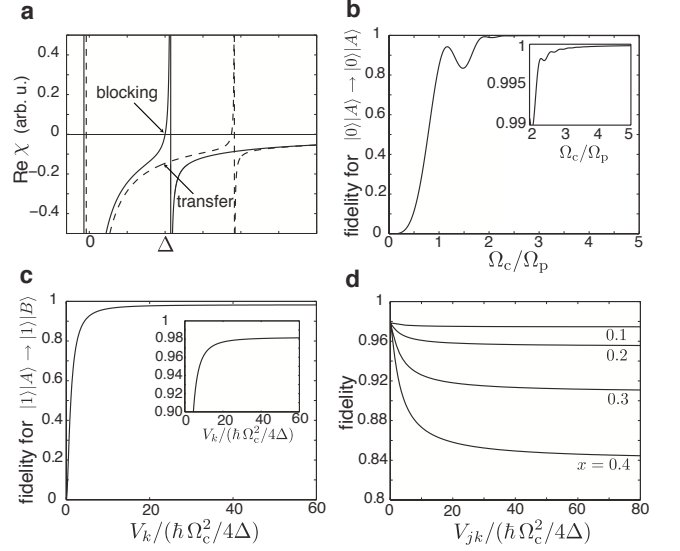


Figure 3: **a**: Linear susceptibility (not to scale) with respect to the Raman laser as a function of the detuning  $\delta$  from the  $|P\rangle$ -level for blocked transfer (solid curve) and in the unblocked case (dashed curve). **b**: Efficiency of the blocking (I) as a function of  $\Omega_c/\Omega_p$ . For  $\Omega_c/\Omega_p > 2$  the transfer of the ensemble atoms from  $|A\rangle$  to  $|B\rangle$  is blocked with more than 99% fidelity. **c**: Efficiency of the Raman transfer in the unblocked situation (II) as a function of the interaction between the control atom and one ensemble atom ( $\Omega_c = 6\Omega_p$ ). **d**: Fidelity of the transfer process  $1/\sqrt{2}(|0\rangle + |1\rangle)|AAA\rangle \rightarrow 1/\sqrt{2}(|0\rangle|AAA\rangle + |1\rangle|BBB\rangle)$  for three ensemble atoms as a function of their interaction strength  $V_{jk}$  and the ratio  $x_{\max} = \sqrt{2}\max(\Omega_p)/\Omega_c$ . We chose the worst case scenario, i.e. all  $V_{jk}$  are equal. The interaction between control atom and ensemble atoms was  $V_k = 10\hbar\Omega_c^2/\Delta$  for all four curves, giving rise to a maximal allowed distance between the control atom and the ensemble atoms of  $2.2\ \mu\text{m}$  ( $1.4\ \mu\text{m}$ ) for the ratio  $x = 0.4$  ( $x = 0.1$ ). We have chosen  $\max(\Omega_p) = 2\pi \times 70\ \text{MHz}$ ,  $\Delta = 2\pi \times 1.2\ \text{GHz}$  in **b-d**, and atomic parameters of  $^{87}\text{Rb}$  (see text).

(I) - *blocking*:  $|0\rangle|A^N\rangle \rightarrow |0\rangle|A^N\rangle$  - If the control atom is initially in state  $|0\rangle$  the first  $\pi$ -pulse has no effect. After adiabatically eliminating the far-detuned  $|P\rangle$  level ( $\Delta \gg \Omega_c, \Omega_p$ ) the effective Hamiltonian of the  $k$ -th ensemble atom reads

$$\frac{H_k}{\epsilon} = x^2 |+\rangle_k \langle +| + |R\rangle_k \langle R| + x \left( |+\rangle_k \langle R| + \text{h.c.} \right), \quad (2)$$

with the characteristic energy scale  $\epsilon = \hbar\Omega_c^2/(4\Delta)$ , the states  $|\pm\rangle = (1/\sqrt{2})[|A\rangle \pm |B\rangle]$  and the rescaled, dimensionless Rabi frequency of the Raman laser  $x(t) = \sqrt{2}\Omega_p(t)/\Omega_c$ . We are interested in the regime where  $x \ll 1$ , in which  $H_k$  describes the EIT scenario [7]. The

solid curve Fig. 3a shows the susceptibility  $\chi(\delta)$  of the system as a function the detuning  $\delta$  from the  $|P\rangle$ -state. We work on two photon-resonance  $\delta = \Delta$  with  $\chi(\Delta) = 0$  and the Raman lasers do not couple to the system. In this case  $H_k$  possesses two dark states given by

$$|d_1\rangle_k = |-\rangle, \quad |d_2\rangle_k = (1 + x^2)^{-1/2}[|+\rangle_k - x|R\rangle_k]. \quad (3)$$

During the smooth Raman pulse the  $k$ -th ensemble atom will adiabatically follow the dark state  $|d\rangle_k = (1/\sqrt{2})[|d_1\rangle_k + |d_2\rangle_k]$ , thereby starting and ending in the state  $|A\rangle_k$ . The remaining (non-dark) states are separated by an energy of at least  $\epsilon$ . This strongly inhibits non-adiabatic losses by Landau-Zener transitions, which limit the fidelity of blocking the transfer and occur with a small probability  $\propto x^6$ . Non-adiabatic couplings to the other dark state are absent. From fig. 3b we see that the transfer is blocked with more than 99% fidelity if  $\Omega_c/\max(\Omega_p(t)) > 2$ . After the second (ineffective)  $\pi$ -pulse on the control atom we have finally performed the step  $|0\rangle|A^N\rangle \rightarrow |0\rangle|A^N\rangle$ .

(II) - *transfer*:  $|1\rangle|A^N\rangle \rightarrow |1\rangle|B^N\rangle$  - If the control atom is initially in state  $|1\rangle$  the first  $\pi$ -pulse transfers the control atom to the Rydberg state  $|r\rangle$ . Since the control and the ensemble atoms interact via  $H_{ce} = \sum_k V_k |r\rangle\langle r| \otimes |R\rangle_k\langle R|$  the Rydberg level of the  $k$ -th ensemble atom is now shifted by the energy  $V_k > 0$  (see fig. 2c). This interaction-induced energy shift lifts the two-photon resonance condition, which is crucial to block the Raman transfer from  $|A\rangle_k$  to  $|B\rangle_k$ . Now, the Raman laser beams no longer address the point of vanishing linear susceptibility  $\chi(\Delta) = 0$  (cf. dashed curve in fig. 3a), but couple far off-resonantly to  $|P\rangle_k$  and thereby realize the transfer of electronic population from  $|A\rangle_k$  to  $|B\rangle_k$ . In fig. 3c the efficiency of the transfer  $|0\rangle|A\rangle_k \rightarrow |1\rangle|B\rangle_k$  is shown as a function of  $V_k$ . Theoretically, ideal transfer is achieved for  $V_k \gg \epsilon$  but even for  $V_k > 40\epsilon$  the efficiency exceeds 98%.

The upper limit for the transfer fidelity is set by three factors. First, the radiative decay from the p-state, which occurs with a probability  $\sim \gamma_p/\Delta \ll 1$  during the Raman transfer. Once the transfer has taken place the control atom is returned to the state  $|1\rangle$  through the second  $\pi$ -pulse, and eventually the step  $|1\rangle|A^N\rangle \rightarrow |1\rangle|B^N\rangle$  is completed [13]. Second, during the Raman laser pulse the control atom resides in the Rydberg state  $|r\rangle$  (lifetime  $\tau_r$ ) for a time  $T$ . In order to minimize the effect of radiative decay from the  $|r\rangle$  state, which reduces the fidelity of the transfer step by the overall factor  $\exp(-T/\tau_r)$  (independently of  $N$ ), the Raman pulse has to be carried out much faster than  $\tau_r$ , i.e  $T < 1\mu s$ . Third, there are mechanical forces which can occur if the control atom *and* the ensemble atom reside in a Rydberg state at a time. This causes entanglement of the internal and external degrees of freedom. However, since the probability for the double occupation of the Rydberg state is  $\propto x^2(\epsilon/V_k)^2$  the corresponding loss of fidelity will be negligibly small.

As the procedure is time-reversal symmetric, the inverse operation  $|0\rangle|A^N\rangle \rightarrow |0\rangle|A^N\rangle$  and  $|1\rangle|B^N\rangle \rightarrow |1\rangle|A^N\rangle$  is accomplished by precisely the same pulse sequence.

Let us now extend the discussion to many interacting ensemble atoms. The ensemble-ensemble interaction  $H_{ee} = \sum_{k>j} V_{jk} |R\rangle_j\langle R| \otimes |R\rangle_k\langle R|$  is of no consequence for transfer step (II) provided that  $V_{jk} \geq 0$  which can be ensured by the proper choice of the Rydberg state  $|R\rangle$ . Since in this step the Rydberg level is anyway shifted by  $H_{ce}$  a further shift by  $H_{ee}$  will have no effect. However, the influence of  $H_{ee}$  on step (I) is more delicate as the blocking of the transfer crucially relies on the EIT condition and hence a destructive interference effect. In fig. 3d we show the fidelity of the process generating the state  $|0\rangle|A^N\rangle + |1\rangle|B^N\rangle$  for three ensemble atoms as a function of their mutual interaction and  $x_{\max} = \sqrt{2}\max(\Omega_p(t))/\Omega_c$ . The fidelity decreases with increasing interaction between the ensemble atoms. Surprisingly, however, the fidelity quickly approaches a constant value as  $V_{jk}$  is further increased. This asymptotic value increases the smaller the parameter  $x_{\max}$ . We will now show that in the limit  $x_{\max} \ll 1$  the blocking of the transfer works with high fidelity, *independently* of the strength of the interaction among the ensemble atoms. Consequently, in this case the maximally achievable fidelity of the full gate operation (1) becomes independent of  $H_{ee}$  and is solely determined by the imperfections discussed in (I) and (II).

The initial state of the ensemble atoms can be written as the direct product of the single particle dark states, which for two atoms takes the form  $|AA(0)\rangle = (1/2)[|d_1d_1\rangle + |d_1d_2\rangle + |d_2d_1\rangle + |d_2d_2\rangle]$ . While the states  $|d_1d_1\rangle$ ,  $|d_1d_2\rangle$  and  $|d_2d_1\rangle$  remain exact dark states for finite  $x(t) \neq 0$ , the state  $|d_2d_2\rangle$  contains a fraction of the two Rydberg state  $|RR\rangle$ , and due to the Rydberg interaction evolves into a new state under the adiabatic time evolution  $x(t)$  denoted as  $|g\rangle$ . This new state acquires an energy shift  $E_g$ , causing a dynamical phase shift which is the dominant mechanism for the suppression of the blocking fidelity. For weak interactions  $V_{jk} \ll \epsilon$  perturbation theory provides the energy shift  $E_g(t) = x^4(t)V_{12}$ , while in the strongly interacting limit  $V_{jk} \gg \epsilon$  it reaches the asymptotic behavior  $E_g(t) \approx 2\epsilon x^4(t)(1 - 2V_{12}^{-1})$ . Consequently, the acquired phase shift is bounded by the worst case scenario of strong interactions with  $V_{jk} \gg \epsilon$ . Then, the 'grey' state  $|g\rangle$  in the present situation with  $\Omega_c \ll \Delta$  reduces to the collective state

$$|g\rangle = (1 + x^4)^{-1/2} [(1 - x^2)|++\rangle - x(|+R\rangle + |R+\rangle)], \quad (4)$$

which has the energy  $E_g(t) = 2\epsilon x^4(t)$ , and contains an admixture of the 'superatom' state  $\frac{1}{\sqrt{2}}(|+R\rangle + |R+\rangle)$  when the Raman lasers are on. During the Raman pulse, the state  $|g\rangle$  acquires the dynamical phase

shift  $2\phi$  with  $\phi = \int_0^T dt E_g(t)/\hbar \approx (35/96)2\pi x_{\max}^2$  [14]. After the Raman pulse we find  $|AA(T)\rangle = (1/2)[|d_1d_1\rangle + |d_1d_2\rangle + |d_2d_1\rangle + e^{-2i\phi}|g\rangle]$ , giving rise to a fidelity of the blocking  $F_b = |\langle AA(0) | AA(T)\rangle|^2 = (1/4)|3 + e^{-2i\phi}|^2$ . The analysis can be generalized for  $N$  ensemble atoms where one finds  $N + 1$  'true' dark states and  $2^N - (N + 1)$  'grey' states, which sustain energy shifts of at most  $\epsilon N(N - 1)x^4(t)$  during the Raman pulse. The fidelity is then

$$F_b = \left| \frac{1}{2^N} \sum_{m=0}^N \frac{N!}{m!(N-m)!} e^{-im(m-1)\phi} \right|^2 \quad (5)$$

with  $\phi \ll 1$  as defined above [10]. Note, that the fidelity can be improved by suppressing the ensemble interaction with a suitable choice of the Rydberg state and/or a cancellation of the leading interaction by the combination of static and microwave fields as was recently proposed for polar molecules [9]. Furthermore, the probability of finding two ensemble atoms in the Rydberg state for strong Rydberg interaction is of the order of  $N^2 x^4 (\min(V_{jk})/\epsilon)^{-2}$ , such that mechanical effects, which might reduce the fidelity, are negligible.

The numbers presented in this work (Fig. 3) have been calculated for  $^{87}\text{Rb}$ . The Rydberg states of the control and the ensemble atoms are 50s and 49s, respectively. The  $C_6$  coefficients of the corresponding Van der Waals interaction have been taken from [11]. The lifetime of the control atom is  $\tau_c = 66 \mu\text{s}$ . The detuning of the Raman laser is  $\Delta = 2\pi \times 1.2 \text{ GHz}$ , the duration of the Raman pulse is  $T = 0.44 \mu\text{s}$  and the decay rate of the intermediate p-level is  $\gamma_p = 36 \text{ MHz}$ . Larger interaction energies and correspondingly larger distances between the control atom and the ensemble atoms can be reached by choosing Rydberg states of higher principal quantum number and/or working with permanent induced dipole moments.

Finally, we briefly comment on the novel possibilities offered by our mesoscopic Rydberg gate in the context of quantum dynamics of atomic condensed matter physics. In Fig. 1 the atomic ensemble can represent cold atoms in an optical lattice as a quantum simulator for a Hubbard model. Since optical lattices can be state dependent, atoms in  $|A\rangle$ , and  $|B\rangle$  can be governed by Hubbard Hamiltonians with different (time-dependent) parameters, generating for an initial quantum state or phase  $|\Phi\rangle$  in the lattice a different time evolution  $U_{A,B}|\Phi\rangle \rightarrow |\Phi_{A,B}\rangle$ . The gate (1) allows the preparation of such mesoscopic superposition of quantum phases on time scales fast compared with the lattice dynamics, entangled with the control atom  $|0\rangle|A^N\rangle|\Phi_A\rangle + |1\rangle|B^N\rangle|\Phi_B\rangle$ . A many particle interferometer, as described in Fig. 4, will provide via measurement of the control atom the overlap  $\langle\Phi_A|\Phi_B\rangle$  [12]. This compares *many body quantum states and their dynamics* on the level of the full wave function, at least of a mesoscopic scale, to be compared with low

order correlation functions accessed in traditional condensed matter and cold atom experiments.

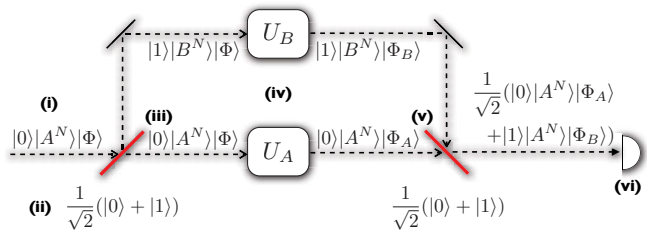


Figure 4: The gate operation (1) represents the fundamental building block of a many-particle interferometer where the overlap of two many-particle wave functions can be measured. (i) Preparation of the initial state. (ii) The control atom is prepared in the superposition  $(1/\sqrt{2})(|0\rangle + |1\rangle)$ . (iii) Gate operation (eq. (1)). (iv) State-dependent evolution. In both interferometer arms a different time evolution, governed by  $U_A$  and  $U_B$ , respectively, takes place. (v) Recombination of the interferometer arms by applying the operation (1). (vi) Measurement of the control atom in the basis  $|c_{\pm}\rangle = (1/\sqrt{2})(|0\rangle \pm |1\rangle)$  yields direct access to the overlap of the two many-body wave functions  $\langle\Phi_A|\Phi_B\rangle = \langle\Phi|U_A^\dagger U_B|\Phi\rangle$ .

M.M. thanks A. Browaeys and P. Grangier for discussions. Support by the Austrian Science Foundation (FWF) through SFB 15, and the EU projects SCALA and NAMEQUAM as well as by the DFG within SFB/TRR21 is acknowledged.

- 
- [1] T. F. Gallagher, *Rydberg Atoms*, Cambridge University Press (1984)
  - [2] D. Jaksch *et al.*, Phys. Rev. Lett. 85, 2208 (2000); M. D. Lukin *et al.*, Phys. Rev. Lett. 87, 037901 (2001); D. Møller, L. B. Madsen and K. Mølmer, Phys. Rev. Lett. 100, 170504 (2008)
  - [3] U. Raitzsch *et al.*, Phys. Rev. Lett. 100, 013002 (2008); M. Reetz-Lamour, T. Amthor, J. Deiglmayr, and M. Weidemüller, Phys. Rev. Lett. 100, 253001 (2008); C. S. van Ditzhuijzen *et al.*, Phys. Rev. Lett. 100, 243201 (2008); T. A. Johnson *et al.*, Phys. Rev. Lett. 100, 113003 (2008); T. Vogt *et al.*, Phys. Rev. Lett. 99, 073002 (2007); D. Tong *et al.*, Phys. Rev. Lett. 93, 063001 (2004)
  - [4] U. Urban *et al.*, arXiv:0805.0758 (2008); A. Gaëtan *et al.*, arXiv:0810.2960 (2008)
  - [5] K. D. Nelson, X. Li and D. S. Weiss, Nature Physics 3, 556 (2007); S. Whitlock, R. Gerritsma, T. Fernholz, R. J. C. Spreeuw, arXiv:0803.2151 (2008)
  - [6] J.-M. Raimond, and S. Haroche, *Exploring the Quantum*, Oxford University Press, Oxford (2006); and references cited.
  - [7] M. Fleischhauer, A. Imamoglu, and J. P. Marangos, Rev. Mod. Phys. 77, 633 (2005); K. J. Weatherill *et al.*, J. Phys. B 41, 201002 (2008)
  - [8] I. Bloch, J. Dalibard, and W. Zwerger, Rev. Mod. Phys. 80, 885 (2008)
  - [9] H. P. Büchler, A. Micheli, and P. Zoller, Nat. Phys. 3, 726 (2007)

- [10] M. Müller *et al.*, unpublished
- [11] K. Singer, J. Stanojevic, M. Weidemüller and Robin Côté, J. Phys. B 38, S295 (2005); <http://quantendynamik.physik.uni-freiburg.de/potcalc.htm>
- [12] P. Zanardi, P. Giorda, and M. Cozzini, Phys. Rev. Lett. 99, 100603 (2007)
- [13] More precisely, the step  $|1\rangle |A^N\rangle \rightarrow -(-1)^N |1\rangle |B^N\rangle$  is realized. The additional phase factor results from the two  $\pi$ -laser pulses on the control atom ( $-1$ ) and trivial phases generated during the Raman transfer of the  $N$  ensemble atoms ( $(-1)^N$ ). This can be avoided by controlling the relative phases of the laser pulses.
- [14] The numerical prefactor stems from the particular choice of the Raman laser profile. We have used  $\Omega_p(t) = \sqrt{(16\pi\Delta)/(3T)} \sin^2(\pi t/T)$ .